Single-electron transfer in metallic nanostructures

Michel H. Devoret, Daniel Esteve & Cristian Urbina

Electrons can be made to pass through a circuit one by one, in nanoscale devices based on the combination of the Coulomb interaction between electrons and their passage by quantum tunnelling through an insulating barrier. Single-electron devices provide a new way of measuring the charge quantum, and clarify how electronic signal processing at the molecular level might function.

ONE individual atom, a purely theoretical entity a hundred years ago, can now be imaged and manipulated at the surface of bulk matter[1] or, free-standing, in vacuum[2]. Is the electron, the simplest and most thoroughly studied particle, amenable to such ultimate control? In vacuum, the detection of single electrons is now routine. A spectacular example of the control of individual electrons travelling in a vacuum chamber is the experiment in which Dehmelt *et al.*[3] were able to probe during three months a single electron kept in an electromagnetic trap, thereby measuring to unprecedented accuracy the anomalous part of its magnetic moment. In matter, the manipulation of individual electrons is a very different game, because the separation between electrons is of the same order as their quantum mechanical wavelength. Here we focus on the most basic type of such manipulation. We explain how it is possible to take, at a precise instant, exactly one electron from a first electrode and transfer it with certainty to a second electrode. By making these electrodes part of an electrical circuit and by continuously repeating this transfer process we can achieve a perfectly controlled current source. In particular, for a sequence of single-electron transfers clocked by a radiofrequency signal at frequency f, the current I will be given simply by $I = ef$ where e is the quantum of charge, a fundamental constant.

Basics of single-charge transfer

Although the charge of the electron was measured as early as 1911 (ref. 4), the granularity of electricity does not usually show up in the macroscopic quantities such as current and voltage, which describe the state of an electric circuit. This is not just a matter of the number of electrons being very large in typical devices. Charge flow in a metal or a semiconductor is a continuous process because conduction electrons are not localized at specific positions. They form a quantum fluid which can be shifted by an arbitrarily small amount. The variations of the charge Q on a capacitor C and of the associated potential difference $U = Q/C$ illustrate this property. The charge Q can be any fraction ε of the charge quantum e: if ρ denotes the electron density in the metallic plates of the capacitor and S their surface area, it is easy to see that a bodily displacement $\delta = \varepsilon/(\rho S)$ of the electronic fluid with respect to the ionic background, in the direction perpendicular to the plates, produces the charge $Q = \varepsilon e$.

There exists, however, a solid-state device in which electric charge flows in a discrete manner. It consists of two metallic electrodes separated by an insulating layer so thin that electrons can traverse it by the tunnel effect[5] (Fig. 1). Tunnelling can be considered as an all-or-nothing process because electrons spend a negligible amount of time under the potential barrier corresponding to the insulating layer[6,7]. If one applies a voltage V to such a tunnel junction, electrons will randomly tunnel across the insulator at a rate given by V/eR_t, where the tunnel resistance R_t is a macroscopic parameter of the junction which depends on the area and thickness of the insulating barrier. Apart from allowing the tunnel effect, the two facing electrodes behave as a capacitor whose capacitance C is the other macroscopic parameter of the junction. It is important to stress that the transport of electrons in a tunnel junction and in a metallic resistor are fundamentally different, even though the current-voltage characteristic is linear in both cases. Charge flows continuously along the resistor, whereas it flows across the junction in packets of e. Obviously, a tunnel junction provides the means to extract electrons one at a time from an electrode. With a single voltage-biased tunnel junction, however, it is not possible to control the instants at which electrons pass from the upstream electrode to the downstream electrode, because of the stochastic nature of tunnelling. A further ingredient is needed.

Suppose that instead of applying directly a voltage source to the junction one biases it with a voltage source U in series with a capacitor C_s (we reserve the letter symbol V for transport voltage sources that have to deliver a static current). A metallic electrode entirely surrounded by insulating material is formed between the junction and the capacitor (Fig. 2*a*). We will call such an isolated electrode, which electrons can enter and leave

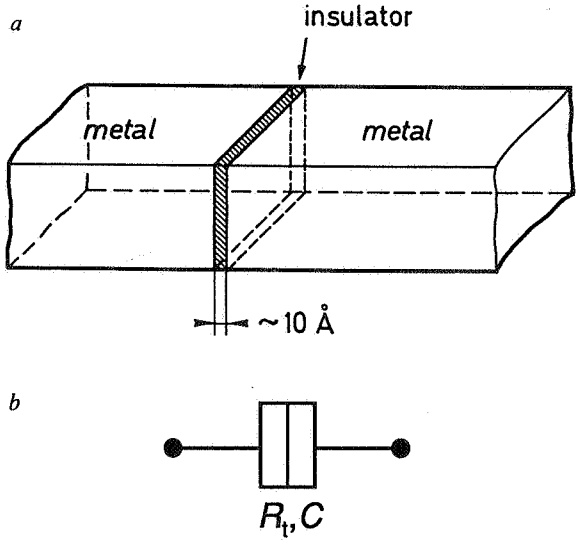

FIG. 1 *a*, Tunnel junction traversed by a current $I(t)$ which consists, when a fixed voltage is imposed to the junction, of uncorrelated charge packets corresponding to individual electrons. Electrons tunnel through the thin layer of insulator sandwiched between the metal electrodes. The junction is represented in circuit schematics by a double box symbol (*b*) and is characterized by the tunnel resistance R_t and capacitance C. It is worth noting that although R_t is called a 'resistance', it characterizes a purely elastic process. At the insulating barrier, the electron wavefunction is partially transmitted and reflected. Its energy does not change. The tunnel resistance is inversely proportional to the barrier transmission coefficient which decreases exponentially with the thickness of the insulating layer. In practice, measurable tunnel resistances can be achieved only with insulating layers a few nanometres thick.

only by tunnelling, an 'island'. The island is coupled electrostatically to the rest of the circuit by the capacitances C and C_s whose charges are denoted by Q and Q_s respectively. Although, as we have seen, Q and Q_s are both continuous variables, their difference is the total excess charge of the island. Because charge can enter the island only by tunnelling, this total charge is a multiple of the electron charge: $Q - Q_s = ne$. Suppose furthermore that the island dimensions are small enough that the electrostatic energy $E_c = e^2/2C_\Sigma$ of one excess electron on the island is much larger than the characteristic energy k_BT of thermal fluctuations. Here, $C_\Sigma = C + C_s$, and k_B and T denote the total capacitance of the island, the Boltzmann constant and the temperature, respectively. This Coulomb energy E_c is the other ingredient of controlled electron transfer.

When $U = 0$, n will stay identically zero because the entrance or exit of an electron would raise the electrostatic energy of the island to a level much higher than permitted by thermal fluctuations. As U increases from zero, however, the total energy difference between the $n = 0$ and $n = 1$ state of the whole circuit decreases, because when an electron tunnels to the island the potential drop C_sU/C_Σ partly compensates the electrostatic energy of the island. In fact, a straightforward calculation of the total energy of the circuit yields $E = E_c(n - C_sU/e)^2$. Thus, when $U = e/2C_s$, the $n = 0$ and $n = 1$ states will have the same energy and an electron can tunnel in and out freely. As U is increased further, the $n = 1$ state becomes the lowest energy state. The maximum stability of the $n = 1$ state against fluctuations is reached at $U = e/C_s$ where, as in the case $U = 0$, and $n = 0$, the charge Q vanishes. It is now easy to see that each time the voltage U is increased by e/C_s, the number n of excess electrons of the island is increased by one. If one plots $\bar{n}$, the average of n, as a function of U, one gets the staircase function shown in Fig. 2*b*. It is therefore possible to control exactly the number of excess electrons of the island by adjusting the voltage U.

As the temperature is increased, the staircase becomes rounded and for temperatures $k_BT \gg E_c$ it approaches the straight dotted line of Fig. 2*b*. In practise, one can reliably cool tunnel junctions down to 50 mK but not much below. To satisfy $E_c \gg k_BT$, C_Σ must be of the order of or smaller than one femtofarad. This requires the fabrication of junctions with typical areas of 50 nm × 50 nm and hence the use of nanofabrication techniques. With such low values of capacitance, the typical voltage corresponding to the addition of an electron is of the order of 100 μV–1 mV, a value which can be easily controlled electronically. To summarize, tunnelling breaks the continuity of the electron fluid into charge packets corresponding to single electrons. The Coulomb energy of excess charges on an island provides a feedback mechanism that regulates the number of electrons tunnelling in and out of the island. At sufficiently low temperature, the exact number of excess electrons on the island does not fluctuate and can be entirely determined by an externally applied voltage. The quenching of the island charge fluctuations for the 'single electron box' (the circuit of Fig. 2*a*) has been demonstrated experimentally by Lafarge *et al.*[8].

We have considered so far only thermal fluctuations of the number n. This variable is also subject to quantum fluctuations. In our analysis of the circuit of Fig. 2*a*, we have neglected the delocalization energy associated with tunnelling. This energy is very small compared with the Coulomb energy. Perturbative calculations[9,10] show that the quantum fluctuations of n become negligible in the limit $R_t \gg R_K = h/e^2$, where h is Planck's constant. The constant $R_K \approx 26\,\text{k}\Omega$ is the resistance quantum. In the next three sections we will consider tunnel barriers sufficiently opaque that this latter condition is fulfilled.

Single electron effects: a brief history

A large class of phenomena exist that combine the partial localization of electrons due to tunnelling and the Coulomb charging energy, and may be called 'single-electron effects'. Decades ago, it was proposed that the variation of the island potential due to the presence of only one excess electron could be large enough to react back on the probability of subsequent tunnelling events[11–15]. At that time, the effect could only be observed in granular metallic materials. It was realized that the hopping of electrons from grain to grain could be inhibited at small voltages if the electrostatic energy of a single electron on a grain was much larger than the energy of thermal fluctuations. The interpretation of these pioneering experiments, in which there is an interplay between single-electron effects and random media properties, was complicated by the limited control over the structure of the sample. With modern nanofabrication techniques, it is possible to design metallic islands of known geometry separated by well-controlled tunnel barriers[16]. This led Fulton and Dolan to perform the first unambiguous demonstration of single-electron effects in an island formed by two junctions[17]. Meanwhile, Likharev and coworkers[18,19] had produced detailed predictions of single-electron effects in a nanoscale current-biased single junction (this system was also considered in refs 20 and 21, but only for junctions in the superconducting state) and proposed various applications of the new effects. This current-biased scheme is analogous in some ways to the circuit of Fig. 2*a*, but with the capacitor replaced by a resistor. In that case there is no island enforcing charge quantization, because an arbitrarily small amount of charge can flow through the resistor. Only the charge on the junction capacitor would provide the feedback of Coulomb energy on tunnelling.

It was later understood that the quantum electromagnetic fluctuations due to the resistor wash out single-electron effects

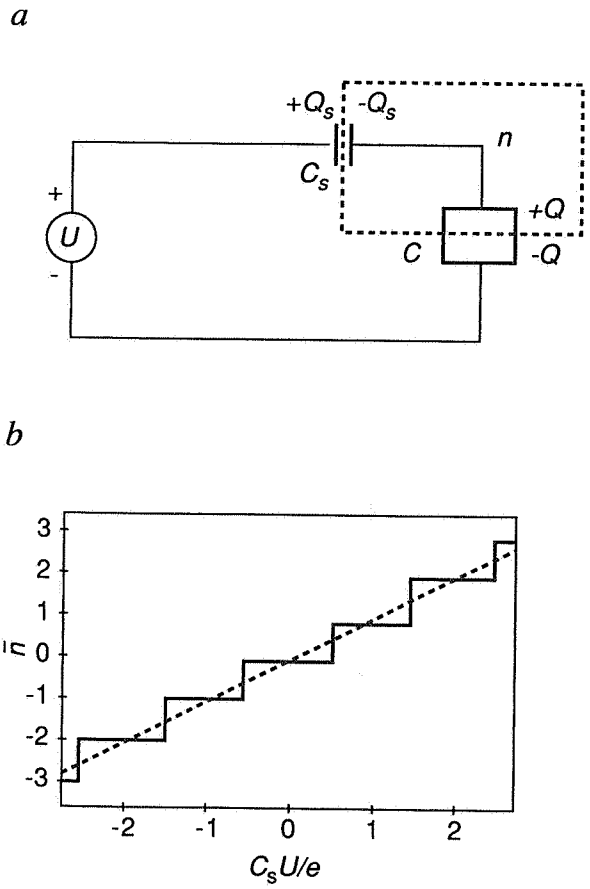

FIG. 2 *a*, Junction biased by a voltage source U in series with a capacitance C_s. The metal electrode between the junction and the capacitance forms an isolated 'island' (box in dashed line) which contains n excess electrons. *b*, Variation of $\bar{n}$, the average of n as a function of U when $k_BT \ll E_c$ (full line) and $k_BT \gg E_c$ (dashed line).

in this single-junction no-island system, unless the resistor is much larger than the resistance quantum R_K up to frequencies of the order of $e^2/(hC)$ (refs 22–24). This has been partially achieved and the competition between single-electron effects and quantum electromagnetic fluctuations has been observed[25,26]. The single-junction no-island system is of interest as an illustration of the foundations of the field, but it is not suited for practical applications because getting rid of quantum electromagnetic fluctuations is so difficult experimentally. In what follows, we will resume the discussion of systems that contain at least one island and are thus immune to quantum electromagnetic fluctuations. We will focus mainly on the controlled transfer of single electrons. For general introductions to single-electron effects in normal and superconducting junction systems, see refs 28–30; for recent snapshots of the state of current research, see refs 31, 32.

The single-electron transistor

The one-junction one-island circuit of Fig. 2*a* is the simplest in which single-electron transfer can occur. On the other hand, it cannot produce an externally measurable static current, as the island is a cul-de-sac for electrons. Let us consider the next order of complexity, the two-junction one-island circuit of Fig. 3*a* (ref. 17). The state of the circuit is now characterized by the two numbers N and N' of electrons having passed through the two junctions. (The sign of N and N' is positive if during tunnelling the electron flows in the direction of increasing voltage, and negative otherwise.) It is convenient to introduce the number $n = N - N'$ of excess electrons on the island and the charge flow index $p = (N + N')/2$. The state $(n, p+1)$ only differs from the state (n, p) in that one electron has been transferred from one terminal of the transport voltage source V to the other. The electrostatic energies of the various capacitances of the circuit are the same. As the precise value of p does not matter here, we will condense the notations (n, p) and $(n, p+1)$ into (n) and $(n)^*$. With regard to the total energy of the circuit, which includes the work of the transport voltage, state $(n)^*$ is lower by eV than state (n) and, hence, the circuit has no absolutely stable states. In principle, a steady current I could flow around the loop formed by the two junctions and the transport voltage V. To go from state (n) to state $(n)^*$, however, the circuit must go through state $(n+1)$ or state $(n-1)$, because tunnel events occur one at a time. States $(n+1)$ and $(n-1)$ differ by state (n) by an electron having tunnelled through the first and second junction, respectively. This is where the single-electron Coulomb energy $E_c = e^2/2C_\Sigma$ comes into play (C_Σ is, as before, the island total capacitance given now by $C_\Sigma = C + C' + C_g$, where C and C' are the two junction capacitances). To simplify the discussion, suppose that $eV \ll E_c$.

When the control 'gate' voltage is set at $U = 0$, the energy of states (-1) and (1) will be $E_c - eV/2 \approx E_c$ above the energy of state (0) (see Fig. 3*c*). At low temperature, this will provide a Coulomb barrier for the transport of electrons around the circuit. In this case the current I should be strictly zero. This situation is called the Coulomb blockade. On the other hand, when the control voltage is such that $C_g U \approx e/2$, states (0) and (1) have nearly the same energy (Fig. 3*c*). As soon as the energy of the (1) state is lowered below that of the (0) state, the $(0) \rightarrow (1)$ transition becomes possible and an electron enters the island through the first junction. If U is such that the energy of the (1) state, although below that of the (0) state, is still above the energy of the $(0)^*$ state, the transition $(1) \rightarrow (0)^*$ takes place and the electron leaves the island through the second junction. Apart from an electron having gone through the device, one is now back to the initial electrostatic state and the cycle can start over again. This cascade of transitions produces a current of order $V/(R_t + R_t')$ through the device (R_t and R_t' are the tunnel resistances of the two junctions). When U is increased further, the energy of the (1) state goes below the energy of the $(0)^*$ state and one enters a new Coulomb blocked state with one excess electron on the island. The domains of the Coulomb blocked states in the set of U values are in a one-to-one correspondance with the flat portions of the staircase of the electron box (Fig. 2*b*) and it is easy to show that, at voltages low compared with the Coulomb voltage E_c/e, the current I is maximum when $C_g U = ne/2$.

In practise, a current of the order of 10^9 electrons per second can be switched on and off by the presence or absence of half the electron charge on the gate capacitor, hence the name 'single electron transistor' (SET) given to this device. The remarkable charge sensitivity of the SET is unrivalled by other devices. (The charge sensitivity of the SET electrometer is six orders of magnitude better than conventional FET electrometers[28]. A possible application is the detection of individual photoinduced electron–hole pairs in semiconductors[33].) But the input capacitance of the SET is, by construction, so tiny that its voltage sensitivity is not high. In this respect, it does not compare favourably with the field effect transistor (FET), the semiconductor device on which most of today's applications of solid-state electronics are based. Furthermore, in the SET the modulation of electron flow by the gate ceases as soon as the bias voltage becomes of the order of the Coulomb gap voltage E_c/e, whereas in the FETs used in digital circuits the modulation of the source–drain current by the gate only saturates at large bias voltages[34]. It is this latter feature which ensures enough voltage gain to compensate

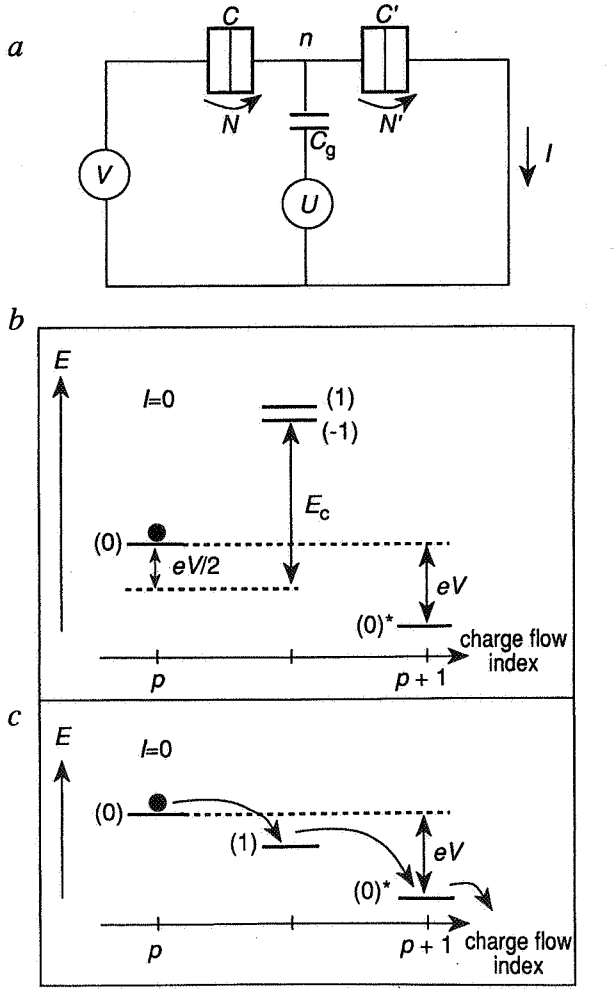

FIG. 3 *a*, Schematic of single-electron transistor (SET). Energy of the states of the circuit when (*b*) $U = 0$ and (*c*) $U = e/C_g$. The numbers in parenthesis are the values of the number n of excess electrons on the SET island. The charge flow index is half the sum of the numbers N and N' of electrons that have traversed the junctions. In (*b*) no current can flow through the device: this is the Coulomb blockade.

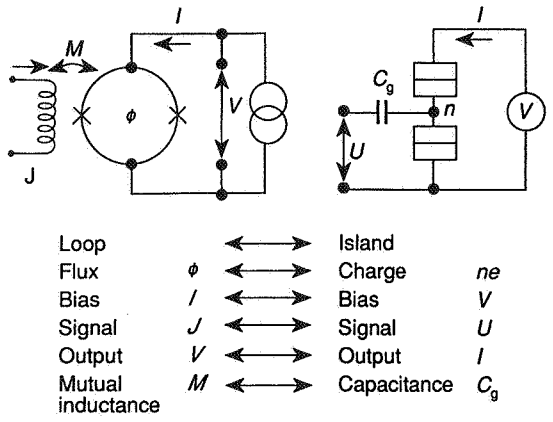

FIG. 4 Comparison between the d.c. SQUID (left) and the SET electrometer (right).

for the dispersion in device parameters and which make robust integrated digital circuit design possible with FETs.

An analogy[28] can be drawn between the SET and the d.c. SQUID with an input coil[35] (see Fig. 4). The d.c. SQUID (superconducting quantum interference device) consists of two Josephson junctions in parallel biased by a static current. In the d.c. SQUID, the output voltage is a periodic function of the current in the input coil, whereas in the SET, the output current is a periodic function of the voltage on the input capacitor. For the d.c. SQUID the period is set by the flux quantum $h/2e$ whereas for the SET the period is set by the charge quantum e. It is tempting to speculate that the SET will play the same role for ultra-sensitive electrometry that the d.c. SQUID plays for ultra-sensitive magnetometry. However, the fundamental impossibility of building the charge analogue of the superconducting flux transformer, which is so crucial to the use of d.c. SQUIDs may severely limit the use of SETs.

The junctions that have been described so far consist in practice of two overlapping metallic films. It is also possible, instead of the three-dimensional gases that conduction electrons form in a metal, to use two-dimensional gases which are found in semiconductor heterostructures such as GaAs/GaAlAs. The detailed manifestations of Coulomb blockade have been thoroughly studied in these systems, where single-electron effects may coexist with the quantum Hall effect[36].

Finally, Coulomb blockade has been observed with a scanning tunnelling microscope (STM) placed over a tiny metallic droplet[37]. The role of the island is played by the droplet. Unfortunately, it has so far been impossible to modulate the gate voltage independently in the droplet–STM systems. On the other hand, very small island dimensions (a few nanometres) can be achieved in this manner, and Coulomb blockade at room temperature has been reported[38]. In principle the island could even be reduced to a single molecule.[39].

Controlled transfer of charges in a circuit

Although the principle of the SET involves the electrostatic energy of a single electron on the SET island, the charge flow through this device is not controlled at the single-electron level. The voltage U controls only the average value of the current. The instants at which electrons pass through the device are random, as in a single junction. A control of the charge flow electron by electron would mean that, using the control voltage U, one would make a single electron enter the island from the left junction, hold it in the island for an arbitrary time and finally make it leave the island through the right junction. One could then go continuously from a Coulomb-blocked state with $n = 0$ to a Coulomb-blocked state with $n = 1$. This is not possible with only one island. When the energy of the (1) state dips below the energy of the (0) state, it is necessarily above the energy of the (0)* state to which it can decay (see Fig. 3*c*). An electron cannot be made to enter the island through one junction without setting the electrostatic energies so that it is energetically favourable for another electron to leave the island through the other junction.

The control of charge flow at the single-electron level requires at least three junctions[9,40]. Let us consider the three-junction two-island circuit of Fig. 5*a*. As in the case of the SET, the state of the circuit can be described using the numbers n_1 and n_2 of excess electrons on each island and the charge flow index given by the third of the algebraic sum of the number of electrons having tunnelled through each junction. Using the condensed notation defined above, (n_1, n_2) and $(n_1, n_2)^*$ denote two states whose charge flow indices differ by one, that is, states differing by an electron which has lost energy eV by passing through the entire device.

We suppose $V \ll \min(e/C_{\Sigma 1}, e/C_{\Sigma 2})$ where $C_{\Sigma 1}$ and $C_{\Sigma 2}$ denote the total capacitances of the two islands. The two control voltages U_1 and U_2, applied to the two gate capacitances C_1 and C_2, allow us to change the relative energy of the various states of this circuit. If we set U_1 and U_2 to $e/2C_1$ and $e/2C_2$ respectively, the energies of states (0, 0), (1, 0), (0, 1) and (0, 0)* form a cascade (Fig. 5b). We are in a situation equivalent to the suppression of Coulomb blockade depicted in Fig. 3*c*, and

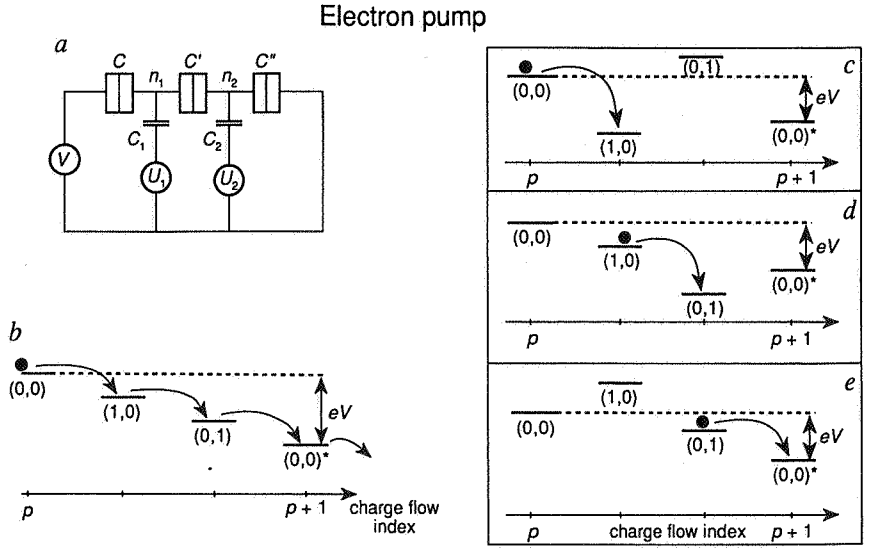

FIG. 5 *a*, Schematic of the single-electron pump. *b*, Energy states of the circuit when the control voltages U_1 and U_2 are set so that Coulomb blockade is suppressed. *c–e*, Pumping cycle which transfers one electron around the circuit of *a*. It is obtained by superposing two phase-shifted modulation signals on the values of U_1 and U_2 corresponding to *b*.

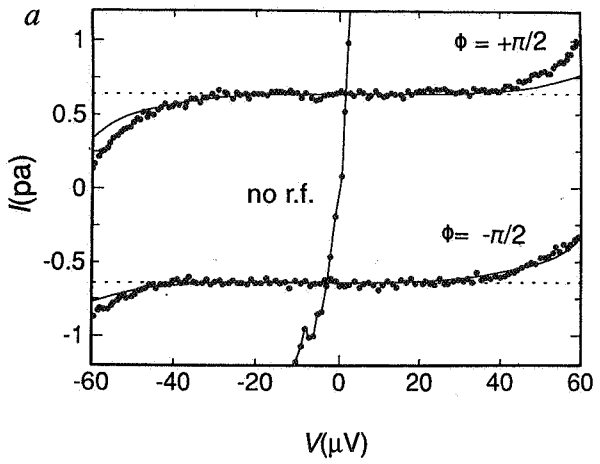

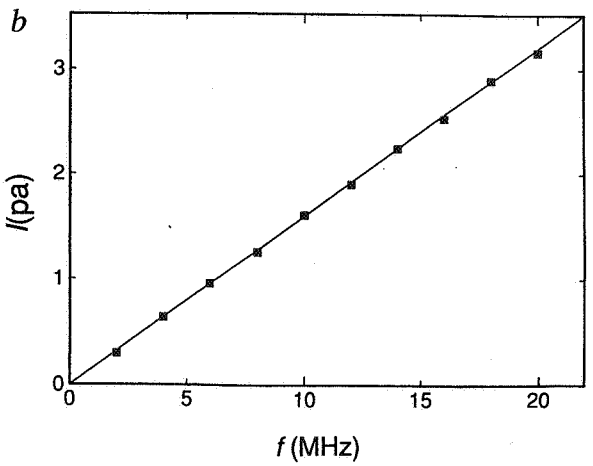

FIG. 6 *a*, Current–voltage characteristic of the pump with and without a $f = 4$ MHz control voltage modulation. The two modulation signals were phase-shifted by Φ. Dashed lines indicate $I = \pm ef$. Full lines are the result of numerical simulations taking into account quantum fluctuations of the island electron number. *b*, Current measured at the inflexion point of the current plateau as a function of the frequency f. Full line is $I = ef$.

a stochastic current flows through the device. Because there are three junctions instead of two, there are now two intermediate states (0, 1) and (1, 0) in the cascade. Each of these states is coupled to (0, 0) or to (0, 0)* but not to both. The lowering of either (0, 1) or (1, 0) below (0, 0) and (0, 0)* stops the stochastic current and puts the circuit in a blocked state. By modulating U_1 and U_2 with dephased periodic signals, the energy of these intermediate states can be cyclically lowered below that of the (0, 0) and (0, 0)* states while avoiding the cascade configuration of Fig. 5*b* (Fig. 5*c*–*e*). One starts from the situation where both (1, 0) and (0, 1) are above (0, 0) and (0, 0)*. The circuit is in a blocked state with no excess electrons on the islands. At first, an increase of U_1 lowers (1, 0) below (0, 0) and (0, 1). An electron goes through the left-most junction and the circuit adopts a new blocked state with an extra electron on the first island (Fig. 5*c*). Then U_2 increases while U_1 decreases: this lowers (0, 1) below (1, 0) and (0, 0)*. A tunnel event consequently takes place through the middle junction and the circuit now adopts a blocked state with an extra electron on the second island (Fig. 5*d*). Finally U_2 is decreased to its initial value, making (0, 1) pass above (0, 0)*. An electron goes through the right-most junction and, apart for a charge e having crossed the entire device, the circuit returns to its initial blocked state (Fig. 5*e*). If the transport voltage V is reversed, the same modulation cycle will still carry electrons in the same direction, provided that the energy difference eV between (0, 0) and (0, 0)* stays small compared with the energy excursions of (0, 1) and (1, 0). The charge now flows in a direction opposite to that imposed by V. Energy conservation is of course not violated. The work done to 'charge' the transport voltage source is provided by the control voltage sources. We have therefore nicknamed this three-junction device the single-electron 'pump'. The pump is reversible: a time-reversed modulation cycle will transfer electrons from right to left.

The actual operation of a physical device is shown in Fig. 6. We first set U_1 and U_2 to the static values $U_1^{dc} = e/C_1$ and $U_2^{dc} = e/C_2$ corresponding to a maximum zero-voltage conductance (centre curve, marked 'no r.f.'). Two periodic signals with the same frequency f but dephased by $\Phi \approx \pi/2$ are then superimposed on the static components U_1^{dc} and U_2^{dc}. This implements the cycle shown in Fig. 5*c*–*e* and a current plateau is obseved (see Fig. 6*a*). One can easily reverse the cycle, leaving all other conditions the same, by changing Φ to $\Phi + \pi$. A current plateau is again observed, with the same absolute value at $V = 0$ but with opposite sign. The height of the plateau is plotted against frequency on Fig. 6*b*. The relation $I = ef$ is well verified, further

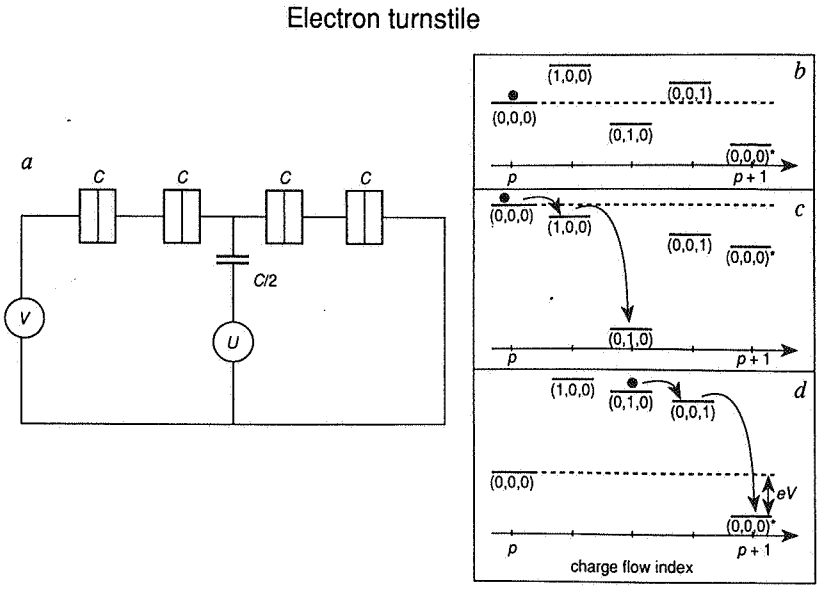

FIG. 7 *a*, Schematic of single-electron turnstile. *b*–*d*, Turnstile cycle which is obtained by modulating the control voltage U and which transfers one electron around the circuit of *a*.

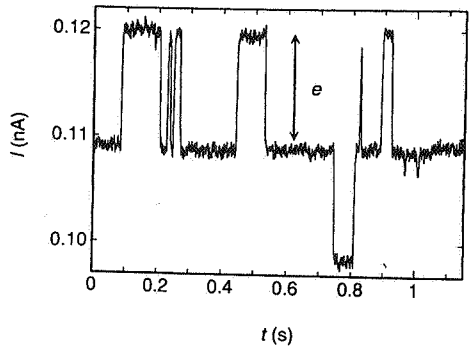

FIG. 8 Time variations of the current through a SET electrometer measuring the charge on an island linked to a charge reservoir through a series of four tunnel junctions. Each jump corresponds to an electron tunnelling into or out of the island.

confirmation that our device does indeed implement the pump principle.

We have seen how two control voltages can transfer electrons one by one in a three-junction device. The transfer of single electron using only one control voltage is possible, but needs at least four junctions. In Fig. 7*a* we show the schematics of a four-junction three-island circuit which we have nicknamed the 'turnstile'[41]. A gate capacitance, with roughly half the value of the capacitance of the junctions, is connected to the central island. Because the gate voltages of the side islands have only to be set to a constant value of zero (in practice, the external gate voltage must be adjusted to compensate for random offset charges[28]), no gate lines have been represented in the figure. The turnstile can be described as a SET with two junctions in the entrance and exit channels. The intermediate islands create energy barriers whose effect is to suppress the stochastic conduction that takes place in the SET for small V, and for U such that $C_gU = e/2$ (see Fig. 7*b–d*). For these conditions, the circuit can exist in two states characterized by the presence or absence of an extra electron on the central island. Suppose one starts with no electron in the central island. As U is increased, all the energies of the intermediate states decrease, although the state with an electron on the central island remains the lowest of the intermediate states (Fig. 7*b*). Consequently, one electron enters the central island. If now one decreases U, all the energies of the intermediate states increase and at one point the state with an extra electron on the central island is no longer the lowest of the intermediate states. An electron then leaves the central island (Fig. 7*d*). It is easy to see that after one cycle of modulation of U, a charge of one electron has passed through the whole device. Like the pump, the turnstile produces a current $I = ef$, where f is the modulation frequency. Unlike the pump, however, the turnstile is an irreversible device, the sign of the current being imposed by the sign of the bias voltage V.

Metrological applications

We have seen that the pump and the turnstile can produce a current determined only by the frequency f and the quantum of charge e. Because frequencies can be accurately determined, these devices would provide in principle a standard of current. The standard is obtained at present by the combination of the Josephson effect[35], which relates a frequency to a voltage through the flux quantum $\Phi_0 = h/2e$, and the quantum Hall effect discovered by von Klitzing[42], which relates current to voltage through the resistance quantum $R_K = h/e^2$. It is important for metrologists to check whether a direct definition of the ampere using the charge quantum e provided by single electron devices would be compatible with the 'Josephson/Klitzing' definition which combines Φ_0 and R_K. The value of the fine-structure constant $\alpha = e^2/(2h\varepsilon_0 c)$, where c and ε_0 denote the speed of light and the electrical permittivity in vacuum, is another important metrological issue that would benefit from the new access to the charge quantum provided by single-electron devices[43]. This latter application would not require direct measurement of the very low current produced by single-electron devices; one would simply charge a calibrated capacitor with a known number of electrons, and compare its voltage with the Josephson volt.

Although the experiments carried out so far to test the precision of the pump and the turnstile are chiefly limited by the precision of current measurements, we should investigate the intrinsic limitations of the devices. One problem is to ensure that the devices are sufficiently cold while passing current. In that respect the pump principle is better than the turnstile, as the pump is reversible and can operate at zero bias voltage[9]. Theoretical analyses show that the fundamental limitation on the accuracy of the devices is due to co-tunnelling events[30,44] during which several tunnel events take place simultaneously on different junctions. These higher-order processes are a manifestation of the quantum fluctuations of island electron number discussed above. Fortunately, it can be demonstrated that the rate of co-tunnelling events decreases exponentially with the number of junctions in a device. Several groups have come to the conclusion that an accuracy better than 10^{-8} in the number of transferred electrons is achievable with a pump with five junctions[45] operating at temperatures of 100 mK or less[46,47]. An important step towards the practical realization of high-accuracy transfer devices is to show experimentally that the number of electrons on an island is well determined when this island is connected to a charge reservoir through several junctions that block the quantum fluctuations of electron number. We have made a direct measurement of the charge of such an island by using a SET electrometer[48]. In Fig. 8 we show single tunnelling events in and out the island occurring on a timescale of a tenth of a second. Although this timescale is still shorter than expected theoretically, we believe that if smaller junctions were used, the spontaneous tunnel rate could be lowered by two orders of magnitude and thus permit metrological experiments.

Future prospects

It has been suggested[27,28] that single-electron devices might find applications in digital electronics. A single electron would code for one bit, obviously the most economical way to store information. In fact, the electron pump is already very similar to the shift registers found in computers. The SET would be the building block of this 'single electronics'. A problem, however, is that metallic SETs made using today's technology have no 'engineer gain': one transistor can barely feed one other transistor in the chain of signal processing, once the dispersions on parameters are accounted for. And no one understands how to get rid of random offset charges[28] which at present ruin any attempt to have more than a few transistors on one chip. In semiconductor devices, single-electron effects may even appear to be a nuisance because they imply that the electrons go through the dots or channels one at a time, a slowing down of the conventional FET operation. The main benefit of understanding single-electron effects in semiconductor nanotechnology may be just to provide the knowledge to fight them efficiently.

The real virtue of single-electron devices, as far as industrial applications are concerned, is that they teach us how to produce digital functions using only tunnelling and the Coulomb interaction, basic ingredients that are available down to the molecular level. In the as yet undeveloped 'molecular electronics' technology[49], basic time constants are very short, there is no dispersion in the parameters of individual components and there are few electrons to work with anyway. There, the principles underlying the devices that have been discussed in this article may be fruitfully implemented. The understanding of single-electron effects may stimulate new research directions in the field of

molecular electronics. And after all, was not the search for the 'philosopher's stone', a premature scientific concept in the Middle Ages, the root of modern chemistry? □

Michel H. Devoret, Daniel Esteve and Cristian Urbina are at the Service de Physique de l'Etat Condensé, CEA-Saclay, 91191 Gif-sur-Yvette cédex, France.

1. Eigler, D. M. & Schweizer, E. K. *Nature* **344,** 524 (1990).
2. Wineland, D. J., Itano, W. M. & Van Dyck, R. S. Jr *Adv. atom. molec. Phys.* **19,** 135 (1983).
3. Van Dyck, R. S. Jr, Schwinberg, P. B. & Dehmelt, H. G. *Phys. Rev.* D**34,** 722 (1986).
4. Millikan, R. A. *Phys. Rev.* **32,** 349 (1911).
5. Solymar, L. *Superconductive Tunneling,* Ch. 2 (Chapman and Hall, London, 1972).
6. Büttiker, M. & Landauer, R. *Phys. Rev. Lett.* **49,** 1739 (1982).
7. Personn, B. N. J. & Baratoff, A. *Phys. Rev.* B**38,** 9616 (1988).
8. Lafarge, P. *et al. Z. Phys.* B**85,** 327 (1981).
9. Esteve, D. *Single Charge Tunneling,* Ch. 3 (ed. Grabert, H. & Devoret, M. H.) (Plenum, New York, 1992).
10. Matveev, K. A. *Zh. eksp. teor. Fiz.* **99,** 1598 (1991); (Engl. transl.) *Sov. Phys. JETP* **72,** 892 (1991).
11. Gorter, C. J. *Physica* **17,** 777 (1951).
12. Neugebauer, C. A. & Webb, M. B. *J. appl. Phys.* **33,** 74 (1962).
13. Giaver, I. & Zeller, H. R. *Phys. Rev. Lett.* **20,** 1504 (1968).
14. Lambe, J. & Jaklevic, R. C. *Phys. Rev. Lett.* **22,** 1371 (1969).
15. Kulik, I. O. & Shekter, R. I. *Zh. eksp. teor. Fiz.* **68,** 623 (1975); (Engl. transl.) *Sov. Phys. JETP* **41,** 308 (1075).
16. Dolan, G. J. & Dunsmuir, J. H. *Physica* B**152,** 7 (1988).
17. Fulton, T. A. & Dolan, G. J. *Phys. Rev. Lett.* **59,** 109 (1987).
18. Likharev, K. K. & Zorin, A. B. *J. low Temp. Phys.* **59,** 347 (1985).
19. Averin, D. V. & Likharev, K. K. *J. low Temp. Phys.* **62,** 345 (1986).
20. Widom, A., Megaloudis, G., Clark, T. D., Prance, H. & Prance, R. J. *J. Phys.* A**15,** 3877 (1982).
21. Ben-Jacob, E. & Gefen, Y. *Phys. Lett.* A**108,** 289 (1985).
22. Nazarov, Yu. V. *Pis'ma Zh. eksp. teor. Fiz.* **49,** 105 (1989); (Engl. transl.) *JETP Lett.* **49,** 126 (1990).
23. Devoret, M. H. *et al. Phys. Rev. Lett.* **64,** 1824 (1990).
24. Girvin, S. M., Glazman, L. I., Jonson, M., Penn, D. R. & Stiles, M. D. *Phys. Rev. Lett.* **64,** 3318 (1990).
25. Cleland, A. N., Schmidt, J. M. & Clarke, *J. Phys. Rev. Lett.* **64,** 1565 (1990).
26. Kuzmin, L. S., Nazarov, Yu. V., Haviland, D. B., Delsing, P. & Claeson, T. *Phys. Rev. Lett.* **67,** 1161 (1991).
27. Likharev, K. K. *IBM J. Res. Dev.* **32,** 144 (1988).
28. Averin, D. V. & Likharev, K. K., in *Quantum Effects in Small Disordered Systems* (eds Altshuler, B. L., Lee, P. A. & Webb, R. A.) (Elsevier, Amsterdam, 1991).
29. Schön, G. & Zaikin, A. D. *Phys. Rep.* **198,** 237 (1990).
30. *Single Charge Tunneling* (eds Grabert, H. & Devoret, M. H.) (Plenum, New York, 1992).
31. *Single Charge Tunneling* spec. Issue *Z. Phys.* B**85,** 317–468 (1991).
32. *Single Electron Tunneling and Mesoscopic Devices, Proc. 4th Int. Conf. SQUID '91* (eds Koch, H. & Lübbig, H.) (Springer, Berlin, 1992).
33. Cleland, A. N., Esteve, D., Urbina, C. & Devoret, M. H. *Appl. Phys. Lett.* (in the press).
34. Fraser, D. A. *The Physics of Semiconductor Devices* (Clarendon, Oxford, 1986).
35. Barone, A. & Paterno, G. *Physics and Applications of the Josephson Effect* (Wiley, New York, 1982).
36. Beenakker, C. W. J. *Single Charge Tunneling,* Ch. 5 (eds Grabert, H. & Devoret, M. H.) (Plenum, New York, 1992).
37. Wilkins, R., Ben-Jacob, E. & Jaklevic, R. D. *Phys. Rev. Lett.* **63,** 801 (1989).
38. Schönenberger, C. *Europhys. Lett.* (in the press).
39. Nejoh, H. *Nature* **353,** 640 (1991).
40. Pothier, H., Lafarge, P., Urbina, C., Esteve, D. & Devoret, M. H. *Physica* B**169,** 573 (1991); *Europhys. Lett.* **17,** 259 (1992).
41. Geerligs, L. J. *et al. Phys. Rev. Lett.* **64,** 2691 (1990).
42. von Klitzing, K. *Rev. mod. Phys.* **58,** 519 (1986).
43. Williams, E. R., Gosh, R. N. & Martinis, J. M. *J. Res. Natn. Inst. Stand Technol.* **97,** (1992).
44. Averin, D. V. & Odintsov, A. A. *Phys. Lett.* A**149,** 251 (1989).
45. Averin, D. V., Odintsov, A. A. & Vyshenskii, S. V. *J. Appl. Phys.* (in the press).
46. Jensen, H. D. & Martinis, J. M. *Phys. Rev.* B**46** (in the press).
47. Pothier, H., Lafarge, P., Esteve, D., Urbina, C. & Devoret, M. H. *IEEE Trans. Magn.* (in the press).
48. Lafarge, P. *et al. C. R. Acad. Sci. Paris* **314,** 883 (1992).
49. Aviram, A. & Ratner, M. *Chem. Phys. Lett.* **29,** 277 (1974); *Molecular Electronic Devices* (ed. Carter, F. L.) (North-Holland, Amsterdam, 1991).

ACKNOWLEDGEMENTS. We thank H. Grabert, P. Joyez, P. Lafarge and H. Pothier for discussions, and P. F. Orfila for help with the figures.

Crystallographic structure and functional implications of the nitrogenase molybdenum–iron protein from *Azotobacter vinelandii*

Jongsun Kim & D. C. Rees*

Division of Chemistry and Chemical Engineering 147-75CH, California Institute of Technology, Pasadena, California 91125, USA

The crystal structure of the nitrogenase molybdenum–iron protein from *Azotobacter vinelandii* has been determined at 2.7 Å resolution. The α- and β-subunits in this $\alpha_2\beta_2$ tetramer have similar polypeptide folds. The FeMo-cofactor is completely encompassed by the α-subunit, whereas the P-cluster pair occurs at the interface between α- and β-subunits. Structural similarities are apparent between nitrogenase and other electron transfer systems, including hydrogenases and the photosynthetic reaction centre

THE enzymatic reduction of dinitrogen to ammonia during biological nitrogen fixation is essential for maintaining the nitrogen cycle on earth. The nitrogenase enzyme system[1–7], which provides the biochemical machinery for nitrogen fixation, consists of two component metalloproteins, the molybdenum iron (MoFe) protein and the iron (Fe) protein. The overall stoichiometry of the biological nitrogen fixation reaction[8]:

$$N_2 + 8H^+ + 8e^- + 16\,Mg\text{–}ATP \rightarrow 2NH_3 + H_2 + 16Mg\text{–}ADP + 16P_i$$

reflects the requirements for reducing equivalents, Mg–ATP and protons, in addition to the two nitrogenase proteins. The Fe-protein is a dimer of two identical subunits coordinating a single 4Fe:4S cluster, whose crystallographic structure has been recently described[9]. The Fe-protein is initially reduced by ferredoxin or flavodoxin *in vivo*, and subsequently transfers electrons to the MoFe-protein in a process that is coupled to the hydrolysis of Mg–ATP. The MoFe-protein is an $\alpha_2\beta_2$ tetramer with a total relative molecular mass of ~240K. The two subunits are of similar size; for example the isolated α and β subunits of *Azotobacter vinelandii* MoFe-protein have 491 and 522 amino acids, respectively[10]. The MoFe-protein contains two types of metal centres, the FeMo-cofactor and P-cluster pair, for which structural models have been recently proposed[11]. In this report, the tertiary and quaternary structures of the MoFe-protein from *A. vinelandii* are presented, based on a 2.7 Å resolution *X*-ray crystallographic analysis. The crystallographic model provides a structural basis for interpreting the functional role of the nitrogenase MoFe-protein in dinitrogen reduction.

* To whom correspondence should be addressed.